# Measurement of top quark polarization in $t\bar{t}$ lepton+jets final states

V.M. Abazov,[31] B. Abbott,[67] B.S. Acharya,[25] M. Adams,[46] T. Adams,[44] J.P. Agnew,[41] G.D. Alexeev,[31] G. Alkhazov,[35] A. Alton[a],[56] A. Askew,[44] S. Atkins,[54] K. Augsten,[7] V. Aushev,[38] Y. Aushev,[38] C. Avila,[5] F. Badaud,[10] L. Bagby,[45] B. Baldin,[45] D.V. Bandurin,[74] S. Banerjee,[25] E. Barberis,[55] P. Baringer,[53] J.F. Bartlett,[45] U. Bassler,[15] V. Bazterra,[46] A. Bean,[53] M. Begalli,[2] L. Bellantoni,[45] S.B. Beri,[23] G. Bernardi,[14] R. Bernhard,[19] I. Bertram,[39] M. Besançon,[15] R. Beuselinck,[40] P.C. Bhat,[45] S. Bhatia,[58] V. Bhatnagar,[23] G. Blazey,[47] S. Blessing,[44] K. Bloom,[59] A. Boehnlein,[45] D. Boline,[64] E.E. Boos,[33] G. Borissov,[39] M. Borysova[l],[38] A. Brandt,[71] O. Brandt,[20] M. Brochmann,[75] R. Brock,[57] A. Bross,[45] D. Brown,[14] X.B. Bu,[45] M. Buehler,[45] V. Buescher,[21] V. Bunichev,[33] S. Burdin[b],[39] C.P. Buszello,[37] E. Camacho-Pérez,[28] B.C.K. Casey,[45] H. Castilla-Valdez,[28] S. Caughron,[57] S. Chakrabarti,[64] K.M. Chan,[51] A. Chandra,[73] E. Chapon,[15] G. Chen,[53] S.W. Cho,[27] S. Choi,[27] B. Choudhary,[24] S. Cihangir[‡],[45] D. Claes,[59] J. Clutter,[53] M. Cooke[k],[45] W.E. Cooper,[45] M. Corcoran,[73] F. Couderc,[15] M.-C. Cousinou,[12] J. Cuth,[21] D. Cutts,[70] A. Das,[72] G. Davies,[40] S.J. de Jong,[29,30] E. De La Cruz-Burelo,[28] F. Déliot,[15] R. Demina,[63] D. Denisov,[45] S.P. Denisov,[34] S. Desai,[45] C. Deterre[c],[41] K. DeVaughan,[59] H.T. Diehl,[45] M. Diesburg,[45] P.F. Ding,[41] A. Dominguez,[59] A. Dubey,[24] L.V. Dudko,[33] A. Duperrin,[12] S. Dutt,[23] M. Eads,[47] D. Edmunds,[57] J. Ellison,[43] V.D. Elvira,[45] Y. Enari,[14] H. Evans,[49] A. Evdokimov,[46] V.N. Evdokimov,[34] A. Fauré,[15] L. Feng,[47] T. Ferbel,[63] F. Fiedler,[21] F. Filthaut,[29,30] W. Fisher,[57] H.E. Fisk,[45] M. Fortner,[47] H. Fox,[39] J. Franc,[7] S. Fuess,[45] P.H. Garbincius,[45] A. Garcia-Bellido,[63] J.A. García-González,[28] V. Gavrilov,[32] W. Geng,[12,57] C.E. Gerber,[46] Y. Gershtein,[60] G. Ginther,[45] O. Gogota,[38] G. Golovanov,[31] P.D. Grannis,[64] S. Greder,[16] H. Greenlee,[45] G. Grenier,[17] Ph. Gris,[10] J.-F. Grivaz,[13] A. Grohsjean[c],[15] S. Grünendahl,[45] M.W. Grünewald,[26] T. Guillemin,[13] G. Gutierrez,[45] P. Gutierrez,[67] J. Haley,[68] L. Han,[4] K. Harder,[41] A. Harel,[63] J.M. Hauptman,[52] J. Hays,[40] T. Head,[41] T. Hebbeker,[18] D. Hedin,[47] H. Hegab,[68] A.P. Heinson,[43] U. Heintz,[70] C. Hensel,[1] I. Heredia-De La Cruz[d],[28] K. Herner,[45] G. Hesketh[f],[41] M.D. Hildreth,[51] R. Hirosky,[74] T. Hoang,[44] J.D. Hobbs,[64] B. Hoeneisen,[9] J. Hogan,[73] M. Hohlfeld,[21] J.L. Holzbauer,[58] I. Howley,[71] Z. Hubacek,[7,15] V. Hynek,[7] I. Iashvili,[62] Y. Ilchenko,[72] R. Illingworth,[45] A.S. Ito,[45] S. Jabeen[m],[45] M. Jaffré,[13] A. Jayasinghe,[67] M.S. Jeong,[27] R. Jesik,[40] P. Jiang[‡],[4] K. Johns,[42] E. Johnson,[57] M. Johnson,[45] A. Jonckheere,[45] P. Jonsson,[40] J. Joshi,[43] A.W. Jung[o],[45] A. Juste,[36] E. Kajfasz,[12] D. Karmanov,[33] I. Katsanos,[59] M. Kaur,[23] R. Kehoe,[72] S. Kermiche,[12] N. Khalatyan,[45] A. Khanov,[68] A. Kharchilava,[62] Y.N. Kharzheev,[31] I. Kiselevich,[32] J.M. Kohli,[23] A.V. Kozelov,[34] J. Kraus,[58] A. Kumar,[62] A. Kupco,[8] T. Kurča,[17] V.A. Kuzmin,[33] S. Lammers,[49] P. Lebrun,[17] H.S. Lee,[27] S.W. Lee,[52] W.M. Lee,[45] X. Lei,[42] J. Lellouch,[14] D. Li,[14] H. Li,[74] L. Li,[43] Q.Z. Li,[45] J.K. Lim,[27] D. Lincoln,[45] J. Linnemann,[57] V.V. Lipaev[‡],[34] R. Lipton,[45] H. Liu,[72] Y. Liu,[4] A. Lobodenko,[35] M. Lokajicek,[8] R. Lopes de Sa,[45] R. Luna-Garcia[g],[28] A.L. Lyon,[45] A.K.A. Maciel,[1] R. Madar,[19] R. Magaña-Villalba,[28] S. Malik,[59] V.L. Malyshev,[31] J. Mansour,[20] J. Martínez-Ortega,[28] R. McCarthy,[64] C.L. McGivern,[41] M.M. Meijer,[29,30] A. Melnitchouk,[45] D. Menezes,[47] P.G. Mercadante,[3] M. Merkin,[33] A. Meyer,[18] J. Meyer[i],[20] F. Miconi,[16] N.K. Mondal,[25] M. Mulhearn,[74] E. Nagy,[12] M. Narain,[70] R. Nayyar,[42] H.A. Neal,[56] J.P. Negret,[5] P. Neustroev,[35] H.T. Nguyen,[74] T. Nunnemann,[22] J. Orduna,[70] N. Osman,[12] A. Pal,[71] N. Parashar,[50] V. Parihar,[70] S.K. Park,[27] R. Partridge[e],[70] N. Parua,[49] A. Patwa[j],[65] B. Penning,[40] M. Perfilov,[33] Y. Peters,[41] K. Petridis,[41] G. Petrillo,[63] P. Pétroff,[13] M.-A. Pleier,[65] V.M. Podstavkov,[45] A.V. Popov,[34] M. Prewitt,[73] D. Price,[41] N. Prokopenko,[34] J. Qian,[56] A. Quadt,[20] B. Quinn,[58] P.N. Ratoff,[39] I. Razumov,[34] I. Ripp-Baudot,[16] F. Rizatdinova,[68] M. Rominsky,[45] A. Ross,[39] C. Royon,[8] P. Rubinov,[45] R. Ruchti,[51] G. Sajot,[11] A. Sánchez-Hernández,[28] M.P. Sanders,[22] A.S. Santos[h],[1] G. Savage,[45] M. Savitskyi,[38] L. Sawyer,[54] T. Scanlon,[40] R.D. Schamberger,[64] Y. Scheglov,[35] H. Schellman,[69,48] M. Schott,[21] C. Schwanenberger,[41] R. Schwienhorst,[57] J. Sekaric,[53] H. Severini,[67] E. Shabalina,[20] V. Shary,[15] S. Shaw,[41] A.A. Shchukin,[34] V. Simak,[7] P. Skubic,[67] P. Slattery,[63] G.R. Snow,[59] J. Snow,[66] S. Snyder,[65] S. Söldner-Rembold,[41] L. Sonnenschein,[18] K. Soustruznik,[6] J. Stark,[11] N. Stefaniuk,[38] D.A. Stoyanova,[34] M. Strauss,[67] L. Suter,[41] P. Svoisky,[74] M. Titov,[15] V.V. Tokmenin,[31] Y.-T. Tsai,[63] D. Tsybychev,[64] B. Tuchming,[15] C. Tully,[61] L. Uvarov,[35] S. Uvarov,[35] S. Uzunyan,[47] R. Van Kooten,[49] W.M. van Leeuwen,[29] N. Varelas,[46] E.W. Varnes,[42] I.A. Vasilyev,[34] A.Y. Verkheev,[31] L.S. Vertogradov,[31] M. Verzocchi,[45] M. Vesterinen,[41] D. Vilanova,[15] P. Vokac,[7] H.D. Wahl,[44] M.H.L.S. Wang,[45] J. Warchol,[51] G. Watts,[75] M. Wayne,[51] J. Weichert,[21] L. Welty-Rieger,[48] M.R.J. Williams[n],[49] G.W. Wilson,[53] M. Wobisch,[54] D.R. Wood,[55] T.R. Wyatt,[41] Y. Xie,[45]

R. Yamada,[45] S. Yang,[4] T. Yasuda,[45] Y.A. Yatsunenko,[31] W. Ye,[64] Z. Ye,[45] H. Yin,[45] K. Yip,[65] S.W. Youn,[45] J.M. Yu,[56] J. Zennamo,[62] T.G. Zhao,[41] B. Zhou,[56] J. Zhu,[56] M. Zielinski,[63] D. Zieminska,[49] and L. Zivkovic[14]

(The D0 Collaboration[*])

[1]*LAFEX, Centro Brasileiro de Pesquisas Físicas, Rio de Janeiro, RJ 22290, Brazil*
[2]*Universidade do Estado do Rio de Janeiro, Rio de Janeiro, RJ 20550, Brazil*
[3]*Universidade Federal do ABC, Santo André, SP 09210, Brazil*
[4]*University of Science and Technology of China, Hefei 230026, People's Republic of China*
[5]*Universidad de los Andes, Bogotá, 111711, Colombia*
[6]*Charles University, Faculty of Mathematics and Physics,*
*Center for Particle Physics, 116 36 Prague 1, Czech Republic*
[7]*Czech Technical University in Prague, 116 36 Prague 6, Czech Republic*
[8]*Institute of Physics, Academy of Sciences of the Czech Republic, 182 21 Prague, Czech Republic*
[9]*Universidad San Francisco de Quito, Quito, Ecuador*
[10]*LPC, Université Blaise Pascal, CNRS/IN2P3, Clermont, F-63178 Aubière Cedex, France*
[11]*LPSC, Université Joseph Fourier Grenoble 1, CNRS/IN2P3,*
*Institut National Polytechnique de Grenoble, F-38026 Grenoble Cedex, France*
[12]*CPPM, Aix-Marseille Université, CNRS/IN2P3, F-13288 Marseille Cedex 09, France*
[13]*LAL, Univ. Paris-Sud, CNRS/IN2P3, Université Paris-Saclay, F-91898 Orsay Cedex, France*
[14]*LPNHE, Universités Paris VI and VII, CNRS/IN2P3, F-75005 Paris, France*
[15]*CEA Saclay, Irfu, SPP, F-91191 Gif-Sur-Yvette Cedex, France*
[16]*IPHC, Université de Strasbourg, CNRS/IN2P3, F-67037 Strasbourg, France*
[17]*IPNL, Université Lyon 1, CNRS/IN2P3, F-69622 Villeurbanne Cedex,*
*France and Université de Lyon, F-69361 Lyon CEDEX 07, France*
[18]*III. Physikalisches Institut A, RWTH Aachen University, 52056 Aachen, Germany*
[19]*Physikalisches Institut, Universität Freiburg, 79085 Freiburg, Germany*
[20]*II. Physikalisches Institut, Georg-August-Universität Göttingen, 37073 Göttingen, Germany*
[21]*Institut für Physik, Universität Mainz, 55099 Mainz, Germany*
[22]*Ludwig-Maximilians-Universität München, 80539 München, Germany*
[23]*Panjab University, Chandigarh 160014, India*
[24]*Delhi University, Delhi-110 007, India*
[25]*Tata Institute of Fundamental Research, Mumbai-400 005, India*
[26]*University College Dublin, Dublin 4, Ireland*
[27]*Korea Detector Laboratory, Korea University, Seoul, 02841, Korea*
[28]*CINVESTAV, Mexico City 07360, Mexico*
[29]*Nikhef, Science Park, 1098 XG Amsterdam, the Netherlands*
[30]*Radboud University Nijmegen, 6525 AJ Nijmegen, the Netherlands*
[31]*Joint Institute for Nuclear Research, Dubna 141980, Russia*
[32]*Institute for Theoretical and Experimental Physics, Moscow 117259, Russia*
[33]*Moscow State University, Moscow 119991, Russia*
[34]*Institute for High Energy Physics, Protvino, Moscow region 142281, Russia*
[35]*Petersburg Nuclear Physics Institute, St. Petersburg 188300, Russia*
[36]*Institució Catalana de Recerca i Estudis Avançats (ICREA) and Institut*
*de Física d'Altes Energies (IFAE), 08193 Bellaterra (Barcelona), Spain*
[37]*Uppsala University, 751 05 Uppsala, Sweden*
[38]*Taras Shevchenko National University of Kyiv, Kiev, 01601, Ukaine*
[39]*Lancaster University, Lancaster LA1 4YB, United Kingdom*
[40]*Imperial College London, London SW7 2AZ, United Kingdom*
[41]*The University of Manchester, Manchester M13 9PL, United Kingdom*
[42]*University of Arizona, Tucson, Arizona 85721, USA*
[43]*University of California Riverside, Riverside, California 92521, USA*
[44]*Florida State University, Tallahassee, Florida 32306, USA*
[45]*Fermi National Accelerator Laboratory, Batavia, Illinois 60510, USA*
[46]*University of Illinois at Chicago, Chicago, Illinois 60607, USA*
[47]*Northern Illinois University, DeKalb, Illinois 60115, USA*
[48]*Northwestern University, Evanston, Illinois 60208, USA*
[49]*Indiana University, Bloomington, Indiana 47405, USA*
[50]*Purdue University Calumet, Hammond, Indiana 46323, USA*
[51]*University of Notre Dame, Notre Dame, Indiana 46556, USA*
[52]*Iowa State University, Ames, Iowa 50011, USA*
[53]*University of Kansas, Lawrence, Kansas 66045, USA*
[54]*Louisiana Tech University, Ruston, Louisiana 71272, USA*
[55]*Northeastern University, Boston, Massachusetts 02115, USA*
[56]*University of Michigan, Ann Arbor, Michigan 48109, USA*

$^{57}$*Michigan State University, East Lansing, Michigan 48824, USA*
$^{58}$*University of Mississippi, University, Mississippi 38677, USA*
$^{59}$*University of Nebraska, Lincoln, Nebraska 68588, USA*
$^{60}$*Rutgers University, Piscataway, New Jersey 08855, USA*
$^{61}$*Princeton University, Princeton, New Jersey 08544, USA*
$^{62}$*State University of New York, Buffalo, New York 14260, USA*
$^{63}$*University of Rochester, Rochester, New York 14627, USA*
$^{64}$*State University of New York, Stony Brook, New York 11794, USA*
$^{65}$*Brookhaven National Laboratory, Upton, New York 11973, USA*
$^{66}$*Langston University, Langston, Oklahoma 73050, USA*
$^{67}$*University of Oklahoma, Norman, Oklahoma 73019, USA*
$^{68}$*Oklahoma State University, Stillwater, Oklahoma 74078, USA*
$^{69}$*Oregon State University, Corvallis, Oregon 97331, USA*
$^{70}$*Brown University, Providence, Rhode Island 02912, USA*
$^{71}$*University of Texas, Arlington, Texas 76019, USA*
$^{72}$*Southern Methodist University, Dallas, Texas 75275, USA*
$^{73}$*Rice University, Houston, Texas 77005, USA*
$^{74}$*University of Virginia, Charlottesville, Virginia 22904, USA*
$^{75}$*University of Washington, Seattle, Washington 98195, USA*
(Dated: July 26, 2016)

We present a study of top quark polarization in $t\bar{t}$ events produced in $p\bar{p}$ collisions at $\sqrt{s} = 1.96$ TeV. Data correspond to 9.7 fb$^{-1}$ collected with the D0 detector at the Tevatron. We use final states containing a lepton and at least three jets. The polarization is measured using the distribution of leptons along the beam and helicity axes, and the axis normal to the production plane. This is the first measurement of top quark polarization at the Tevatron in $\ell$+jets final states, and first measurement of transverse polarization in $t\bar{t}$ production. The observed distributions are consistent with the standard model.

The standard model (SM) predicts that top quarks produced at the Tevatron collider are almost unpolarized, while models beyond the standard model (BSM) predict enhanced polarizations [1].

The top quark polarization $P_{\hat{n}}$ can be measured in the top quark rest frame through the angular distribution of the top quark decay products relative to some chosen axis $\hat{n}$ [2]:

$$\frac{1}{\Gamma}\frac{d\Gamma}{d\cos\theta_{i,\hat{n}}} = \frac{1}{2}(1 + P_{\hat{n}}\kappa_i \cos\theta_{i,\hat{n}}), \qquad (1)$$

where $i$ is the decay product (lepton, quark, or neutrino), $\kappa_i$ is its spin analyzing power ($\approx 1$ for charged leptons, 0.97 for $d$-type quarks, $-0.4$ for $b$-quarks, and $-0.3$ for

*with visitors from $^a$Augustana College, Sioux Falls, SD 57197, USA, $^b$The University of Liverpool, Liverpool L69 3BX, UK, $^c$Deutshes Elektronen-Synchrotron (DESY), Notkestrasse 85, Germany, $^d$CONACyT, M-03940 Mexico City, Mexico, $^e$SLAC, Menlo Park, CA 94025, USA, $^f$University College London, London WC1E 6BT, UK, $^g$Centro de Investigacion en Computacion - IPN, CP 07738 Mexico City, Mexico, $^h$Universidade Estadual Paulista, São Paulo, SP 01140, Brazil, $^i$Karlsruher Institut für Technologie (KIT) - Steinbuch Centre for Computing (SCC), D-76128 Karlsruhe, Germany, $^j$Office of Science, U.S. Department of Energy, Washington, D.C. 20585, USA, $^k$American Association for the Advancement of Science, Washington, D.C. 20005, USA, $^l$Kiev Institute for Nuclear Research (KINR), Kyiv 03680, Ukraine, $^m$University of Maryland, College Park, MD 20742, USA, $^n$European Orgnaization for Nuclear Research (CERN), CH-1211 Geneva, Switzerland and $^o$Purdue University, West Lafayette, IN 47907, USA. $^{\ddagger}$Deceased.

neutrinos and $u$-type quarks [3]), and $\theta_{i,\hat{n}}$ is the angle between the direction of the decay product $i$ and the quantization axis $\hat{n}$. The mean polarizations of the top and antitop quarks are expected to be identical because of CP conservation. The quantization axes are defined in the $t\bar{t}$ rest frame, while the decay product directions are defined after successively boosting the particles to the $t\bar{t}$ rest frame and then to the parent top quark rest frame. We measure the polarization along three quantization axes: (i) **beam axis** $\hat{n}_p$, given by the direction of the proton beam [2], (ii) **helicity axis** $\hat{n}_h$, given by the direction of the parent top and antitop quark, and (iii) **transverse axis** $\hat{n}_T$, given as perpendicular to the production plane defined by the proton and parent top (or antitop) quark directions, i.e., $\hat{n}_p \times (-)\hat{n}_{t(\text{or }\bar{t})}$ [4, 5].

The top quark polarization along the helicity axis was previously studied in $p\bar{p}$ collisions by the D0 collaboration [6] as part of the measurement of angular asymmetries of leptons. Recently, D0 measured the top quark polarization along the beam axis in $t\bar{t}$ final states with two leptons [7], and it was found to be consistent with the SM. The ATLAS and CMS collaborations measured the top quark polarization in $pp$ collisions along the helicity axis, and the results are consistent with no polarization [8, 9]. The Tevatron and the LHC polarizations are expected to be different because of the difference in the initial states, which provides motivation [10, 11] for measuring polarizations in Tevatron data. For beam and transverse axes, the $p\bar{p}$ polarization are expected to be larger than those for $pp$ [2, 4], therefore offering greater sensitivity.

The longitudinal polarizations along the beam and helicity axes at the Tevatron collider are predicted by the SM to be $(-0.19 \pm 0.05)\%$ and $(-0.39 \pm 0.04)\%$ [12], respectively, while the transverse polarization is estimated to be $\approx 1.1\%$ [5]. Observation of a significant departure from the expected value would be evidence for BSM contributions [1].

We present a measurement of top quark polarization in $\ell$+jets final states of $t\bar{t}$ production. The lepton is most sensitive to the polarization and is easily identified. We therefore examine the angular distribution of leptons. After selecting the events in the $\ell$+jets final state, we perform a kinematic fit to reconstruct the lepton angles relative to the various axes. The resulting distributions are fitted with mixtures of signal templates with $+1$ and $-1$ polarizations to extract the observed values. The down-type quark has an analyzing power close to unity, but its identification is difficult. It is therefore not used in the measurement. However, to gain statistical precision we use reweighted Monte Carlo (MC) down-type quark distributions in forming signal event templates.

We analyze data collected by the D0 detector, corresponding to an integrated luminosity of 9.7 fb$^{-1}$ of $p\bar{p}$ collisions at $\sqrt{s} = 1.96$ TeV. The D0 central tracking system consists of a silicon microstrip tracker and a central fiber tracker surrounding the interaction region up to detector pseudorapidities [13] $|\eta_d| \approx 3$ and $|\eta_d| \approx 2.5$, respectively. The central-tracking system, located within a 1.9 T superconducting solenoidal magnet [14, 15], provides measurements for tracking and vertexing. A liquid-argon calorimeter with uranium absorber plates has a central section covering pseudorapidities up to $|\eta_d| \approx 1.1$, and two end calorimeters that extend coverage to $|\eta_d| \approx 4.2$, with all three housed in separate cryostats [16]. An outer muon system, which covers $|\eta_d| < 2$, consists of a layer of tracking detectors and scintillation trigger counters in front of 1.8 T iron toroids, followed by two similar layers after the toroids [17].

Each top quark of the $t\bar{t}$ pair decays into a $b$ quark and a $W$ boson with nearly 100% probability, leading to a $W^+W^-b\bar{b}$ final state. In $\ell$+jets events, one of the $W$ bosons decays leptonically and the other into quarks that evolve into jets. The trigger selects $\ell$+jets events with at least one lepton, electron ($e$) or a muon ($\mu$), with efficiency of 95% or 80% for $t\bar{t}$ events containing reconstructed $e$ or $\mu$ candidates, respectively. This analysis requires the presence of one isolated $e$ [18] or $\mu$ [19] with transverse momentum $p_T > 20$ GeV and physics pseudorapidity [13] $|\eta| < 1.1$ or $|\eta| < 2$, respectively. In addition, leptons are required to originate from within 1 cm of the primary $p\bar{p}$ interaction vertex (PV) in the coordinate along the beam axis. Accepted events must have a reconstructed PV within 60 cm of the center of the detector along the beam axis. Furthermore, we require an imbalance in transverse momentum $\not{p}_T > 20$ GeV, expected from the undetected neutrino. Jets are reconstructed us-

ing an iterative cone algorithm [20] with a cone parameter of $R = 0.5$. Jet energies are corrected to the particle level using calibrations from studies of exclusive $\gamma$+jet, $Z$+jet, and dijet events [21]. These calibrations account for differences in detector response to jets originating from gluons, $b$ quarks, and $u, d, s$, or $c$ quarks. We require at least three jets with $p_T > 20$ GeV within $|\eta| < 2.5$, and $p_T > 40$ GeV for the jet of highest $p_T$. At least one jet per event is required to be identified as originating from a $b$ quark ($b$ tagged) through the use of a multivariate algorithm [22]. In $\mu$+jets events, upper limits are required on the transverse mass of the reconstructed $W$ boson [23] of $M_T^W < 250$ GeV and $\not{p}_T < 250$ GeV to remove events with misreconstructed muon $p_T$. Additional selections are applied to reduce backgrounds in muon events, and to suppress contributions from multijet production. A detailed description of these requirements can be found in Ref. [24]. In addition, we require the curvature of the track associated with the lepton to be well measured to reduce lepton charge misidentification.

We use MC simulated $t\bar{t}$ events generated at the next-to-leading-order (NLO) in perturbative quantum chromodynamics (QCD) using the MC@NLO event generator version 3.4 [25] or the leading-order (LO) ALPGEN event generator version 2.11 [26]. Parton showering, hadronization, and modeling of underlying event are performed with HERWIG [27] for MC@NLO events and with PYTHIA 6.4 [28] for ALPGEN events. The detector response is simulated using GEANT3 [29]. To model the effects of multiple $p\bar{p}$ interactions, the MC events are overlaid with events from random $p\bar{p}$ collisions with the same luminosity distribution as data. The main background to the $t\bar{t}$ signal is $W$+jets events, where the $W$ boson is produced via the electroweak interaction together with additional partons from QCD radiation. The $W$+jets final state can be split into four subsamples according to parton flavor: $Wb\bar{b}$ + jets, $Wc\bar{c}$ + jets, $Wc$ + jets, and $W$+light jets, where light refers to gluons, $u$, $d$, or $s$ quarks. The $W$+jets background is modeled with ALPGEN and PYTHIA [26, 28], as is the background from $Z$+jets events. Other background processes include $WW$, $WZ$, and $ZZ$ diboson productions simulated using PYTHIA, and single top quark electroweak production simulated using COMPHEP [30]. The multijet background, where a jet is misidentified as an isolated lepton, is estimated from the data using the matrix method [24, 31]. We use six different BSM models [32] to study modified $t\bar{t}$ production: one $Z'$ boson model and five axigluon models with different axigluon masses and couplings (m200R, m200L, m200A, m2000R, and m2000A, where L, R, and A refer to left-handed, right-handed, and axial couplings, and numbers are the particle masses in GeV). The BSM events are generated with LO MADGRAPH 5 [33] interfaced to PYTHIA for parton evolution.

A constrained kinematic $\chi^2$ fit is used to associate the observed leptons and jets with the individual top quarks

using a likelihood term for each jet-to-quark assignment, as described in Ref. [34]. We assume the four jets with largest $p_T$ to originate from $t\bar{t}$ decay in events with more than four jets. The algorithm includes a technique that reconstructs events with a lepton and only three jets [35]. The addition of the three-jet sample almost doubles the signal sample as shown in Table I. In our analysis, all possible assignments of jets to final state quarks are considered and weighted by the $\chi^2$ probability of each kinematic fit and by the $b$ tagging probability.

To determine the sample composition, we construct a kinematic discriminant based on the approximate likelihood ratio of expectations for $t\bar{t}$ and $W$+jets events [36]. The input variables are chosen to achieve good separation between $t\bar{t}$ and $W$+jets events, and required to be well modeled and not strongly correlated with one another or with the lepton polar angles used in the measurement. Sets of input variables are selected independently for the $\ell + 3$ jet and the $\ell + \geq 4$ jet events, each in 3 subchannels according to the number of $b$ tagged jets: 0, 1, $\geq 2$. The channels without $b$ tagged jets are used to determine the sample composition and background calibration, not to measure the polarization.

The input variables used for the $\ell + 3$ jet kinematic discriminant are: $k_T^{min} = \min(p_{T,a}, p_{T,b}) \cdot \Delta R_{ab}$, where $\Delta R_{ab} = \sqrt{(\eta_a - \eta_b)^2 + (\phi_a - \phi_b)^2}$ is the angular distance between the two closest jets ($a$ and $b$), $\min(p_{T,a}, p_{T,b})$ represents the smaller transverse momentum of the two jets, and the $\phi$ are their azimuths in radians; aplanarity, $A = 3/2\lambda_3$, where $\lambda_3$ is the smallest eigenvalue of the normalized momentum tensor; $H_T^\ell$, the scalar sum of the $p_T$ of the jets and lepton; $\Delta R$ between the leading jet and the next-to-leading jet; and $\Delta R$ between the lepton and the leading jet.

The input variables for the $\ell + \geq 4$ jet discriminant are: $k_T^{min}$; aplanarity; $H_T^\ell$; centrality, $C = H_T/H$, where $H_T$ is the scalar sum of all jet $p_T$ values, and $H$ is the scalar sum of all jet energies; the lowest $\chi^2$ among the different kinematic fit solutions in each event; $(p_T^{b_{\mathrm{had}}} - p_T^{b_{\mathrm{lep}}})/(p_T^{b_{\mathrm{had}}} + p_T^{b_{\mathrm{lep}}})$, the relative $p_T$ difference between $b_{\mathrm{lep}}$, the $b$ jet candidate from the $t \to b\ell\nu$ decay, and $b_{\mathrm{had}}$, the $b$ jet candidate from the $t \to bqq'$ decay; and $m_{jj}$, the invariant mass of the two jets corresponding to the $W \to q\bar{q}'$ decay.

The sample composition is determined from a simultaneous maximum-likelihood fit to the kinematic discriminant distributions. The $W$+jets background is normalized separately for the heavy-flavor contribution ($Wb\bar{b}$ + jets and $Wc\bar{c}$ + jets) and for the light-parton contribution ($Wc$ + jets and $W$+light jets). The sample composition after implementing the selections, and fitting the maximum-likelihood to data, is broken down into individual channels by lepton flavor and number of jets, and summarized in Table I. The obtained $t\bar{t}$ yield is close to the expectations.

| Source | 3 jets | | $\geq$ 4 jets | |
|---|---|---|---|---|
| | $e$+jets | $\mu$+jets | $e$+jets | $\mu$+jets |
| $W$+jets | $1741 \pm 26$ | $1567 \pm 15$ | $339 \pm 3$ | $295 \pm 3$ |
| Multijet | $494 \pm 7$ | $128 \pm 3$ | $147 \pm 4$ | $49 \pm 2$ |
| Other Bkg | $446 \pm 5$ | $378 \pm 2$ | $87 \pm 1$ | $73 \pm 1$ |
| $t\bar{t}$ signal | $1200 \pm 25$ | $817 \pm 20$ | $1137 \pm 24$ | $904 \pm 23$ |
| Sum | $3881 \pm 37$ | $2890 \pm 25$ | $1710 \pm 25$ | $1321 \pm 23$ |
| Data | $3872$ | $2901$ | $1719$ | $1352$ |

TABLE I: Sample composition and event yields after implementing the selection requirements and the maximum likelihood fit to kinematic distributions in data. Only statistical uncertainties are shown.

The lepton angular distributions in $W$+jets events must be well-modeled since these events form the leading background, especially in the $\ell + 3$ jet sample. We therefore use a control sample of $\ell + 3$ jet events without $b$ tagged jets, as such events are dominated by $W$+jets. We reweight the $W$+jets MC events so that the $\cos\theta_{\ell,\hat{n}}$ distributions agree with those for the control events in data. The correction to MC obtained from the control sample is propagated to the data sample of the measurement, which provides corrections of 0.047 for polarization along the beam axis, 0.011 for the transverse axis, and a negligible amount for the helicity axis. We observe the $W$+jets events to have polarization of $+0.18$ along beam axis, $-0.23$ along helicity axis, and $-0.02$ along transverse axis. Other backgrounds count for polarization of $+0.05$ (beam axis), $-0.30$ (helicity axis), and $+0.01$ (transverse axis).

To measure the polarization, a fit is performed to the reconstructed $\cos\theta_{\ell,\hat{n}}$ distribution using $t\bar{t}$ templates of $+1$ and $-1$ polarizations, and background templates normalized to the expected event yield. The signal templates arise from the $t\bar{t}$ MC sample generated with no polarization but reweighted to follow the expected double differential distribution [2]:

$$\frac{1}{\Gamma}\frac{d\Gamma}{d\cos\theta_1 \cos\theta_2} = \frac{1}{4}(1 + \kappa_1 P_{\hat{n},1}\cos\theta_1 + \rho\kappa_2 P_{\hat{n},2}\cos\theta_2 - \kappa_1\kappa_2 C\cos\theta_1\cos\theta_2), \quad (2)$$

where indices 1 and 2 represent the $t$ and $\bar{t}$ quark decay products (the leptons and down quarks, or their charge conjugates) $\kappa$ is the spin-analyzing power, and $C$ is the $t\bar{t}$ spin correlation coefficient for a given quantization axis. We use the SM values $C = -0.368$ (helicity axis) and $C = 0.791$ (beam axis), both calculated at NLO in QCD and in electroweak couplings in Ref. [2]. The spin correlation factor is not known for the transverse axis, and thus we set $C = 0$. The $P_{\hat{n},i}$ represents the polarization state we model (here $P_{\hat{n},i} = \pm 1$) along the chosen axis $\hat{n}$. In the SM, assuming CP invariance, $P_{\hat{n},1} = P_{\hat{n},2}$ and gives the relative sign factor $\rho$ a value of $+1$ for the helicity axis and $-1$ for the beam and transverse axes [2].

A simultaneous fit is performed for the eight samples defined according to lepton flavor ($e$ or $\mu$), lepton charge, and number of jets (3 or $\geq 4$). The observed polarization is taken as $P = f_+ - f_-$, where $f_\pm$ are the fraction of events with $P = +1$ and $-1$ returned from the fit. The fitting procedure and methodological approach are verified using pseudo-experiments for five values of polarization, and through a check of consistency with predictions, using the BSM models with non-zero generated longitudinal polarizations. The fitted polarizations and the model inputs are in good agreement, thus verifying our template methodology. The distributions in the cosine of the polar angle of leptons from $t\bar{t}$ decay for all three axes are shown in Fig. 1.

A previous measurement of top quark polarization and the forward-backward $t$ and $\bar{t}$ asymmetry in dilepton final states [7] noted a correlation between these two measurements. This correlation is caused by acceptance and resolution effects in the kinematic reconstruction of the events. We determine the dependence of the observed polarization on the forward-backward asymmetry at the parton level, $A_{\text{FB}}$, using samples in which the $t$ and $\bar{t}$ rapidity distributions are reweighted to accommodate the polarizations. We then use a correction for the difference between the nominal MC@NLO production-level $A_{\text{FB}}$ of $(5.01 \pm 0.03)\%$ and the NNLO calculation [37] of $(9.5 \pm 0.7)\%$. The observed correction is $-0.030$ for the polarization along the beam axis, less than 0.002 for the polarization along the helicity axis, and is negligible for the transverse polarization. The uncertainty on the expected $A_{\text{FB}}$ is propagated to the measurement as part of the methodology systematic uncertainty.

We have evaluated several categories of systematic uncertainties using fully simulated events: uncertainties associated with jet reconstruction, jet energy measurement, $b$ tagging, modeling of background and signal events, parton distribution functions (PDFs), and those associated with procedures and assumptions made in the analysis. The sources of systematic uncertainties and their contributions are listed in Table II. Details about the evaluation of the uncertainties can be found in Ref. [24, 34]. Additionally, we assign an uncertainty in modeling the invariant mass of the $t\bar{t}$ system ($m_{t\bar{t}}$) based on the difference in $m_{t\bar{t}}$ distributions in our signal MC and the NNLO predictions [38].

The measured polarizations for the three spin quantization axes are shown in Table III. Results on the longitudinal polarizations are presented in Fig. 2 and compared to SM predictions and several of the BSM models discussed previously. The measurement along the beam axis is consistent with the previous D0 result in the dilepton channel [7], $P = 0.113 \pm 0.093$. We estimate the correlation between this result for beam axis and that of Ref. [7] to be 5%. The combination using the method of Refs. [39, 40] yields a top quark polarization along the beam axis $P = 0.081 \pm 0.048$.

| Source | Beam | Helicity | Transverse |
|---|---|---|---|
| Jet reconstruction | $\pm0.010$ | $\pm0.008$ | $\pm0.008$ |
| Jet energy measurement | $\pm0.010$ | $\pm0.023$ | $\pm0.006$ |
| $b$ tagging | $\pm0.009$ | $\pm0.014$ | $\pm0.005$ |
| Background modeling | $\pm0.007$ | $\pm0.021$ | $\pm0.004$ |
| Signal modeling | $\pm0.016$ | $\pm0.020$ | $\pm0.008$ |
| PDFs | $\pm0.013$ | $\pm0.011$ | $\pm0.003$ |
| Methodology | $\pm0.013$ | $\pm0.007$ | $\pm0.004$ |
| Total systematic uncertainty | $\pm0.030$ | $\pm0.042$ | $\pm0.015$ |
| Total statistical uncertainty | $\pm0.046$ | $\pm0.044$ | $\pm0.030$ |
| Total uncertainty | $\pm0.055$ | $\pm0.061$ | $\pm0.034$ |

TABLE II: Summary of the uncertainties in the measured top quark polarization along three axes. The numbers indicate difference in polarization when the measurement is repeated using alternative modeling, after applying uncertainties from the employed methods, or from assumptions made in the measurement.

| Axis | Measured polarization | SM prediction |
|---|---|---|
| Beam | $+0.070 \pm 0.055$ | $-0.002$ |
| Beam - D0 comb. | $+0.081 \pm 0.048$ | $-0.002$ |
| Helicity | $-0.102 \pm 0.061$ | $-0.004$ |
| Transverse | $+0.040 \pm 0.034$ | $+0.011$ |

TABLE III: Measured top quark polarization from the $t\bar{t}$ $\ell$+jet channel along the beam, helicity, and transverse axes. And the combined polarization for beam axis with the dilepton result by D0. The total uncertainties are obtained by adding the statistical and systematic uncertainties in quadrature.

In summary, we measure the top quark polarization for $t\bar{t}$ production in $p\bar{p}$ collisions at $\sqrt{s} = 1.96$ TeV along several spin-quantization axes. The polarizations are consistent with SM predictions. The transverse polarization is measured for the first time. These are the most precise measurements of top quark polarization in $p\bar{p}$ collisions.
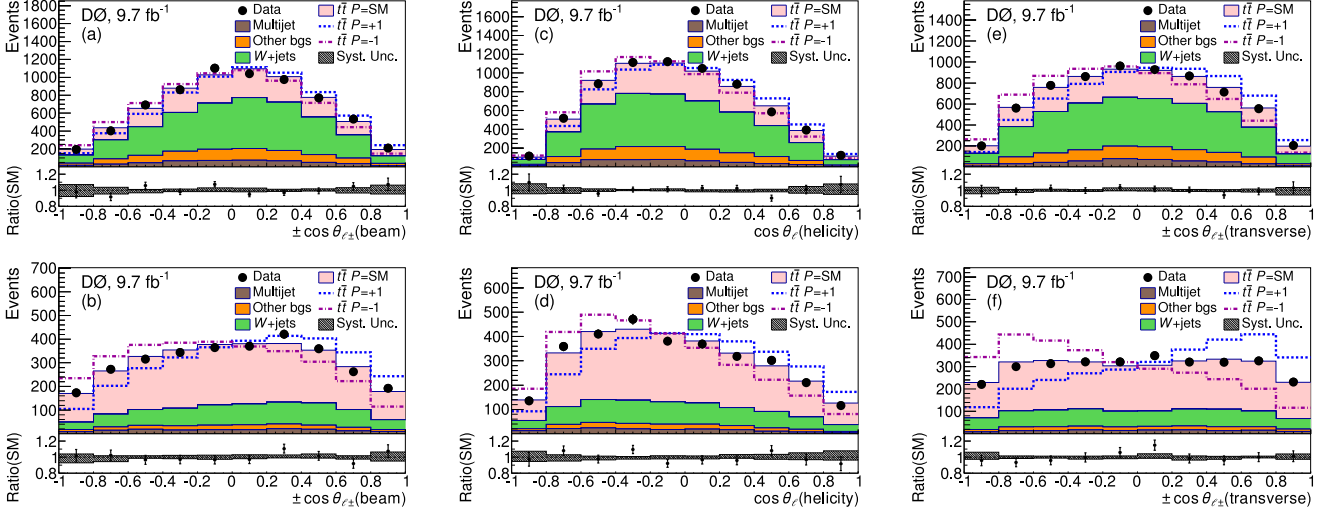
FIG. 1: (color online) The combined $e$+jets and $\mu$+jets $\cos\theta$ distributions for data, expected backgrounds, and signal templates for $P = -1$, SM, and +1. Panels (a), (c), and (e) show $\ell$+3 jet events; (b), (d), and (f) show $\ell+ \geq 4$ jet events; (a) and (b) show distributions relative to the beam axis; (c) and (d) show distributions relative to the helicity axis; and (e) and (f) show distributions relative to the transverse axis. The hashed areas represent systematic uncertainties. The direction of the $\cos\theta$ axis is reversed for the $\ell^-$ events for beam and transverse spin quantization axes plots.
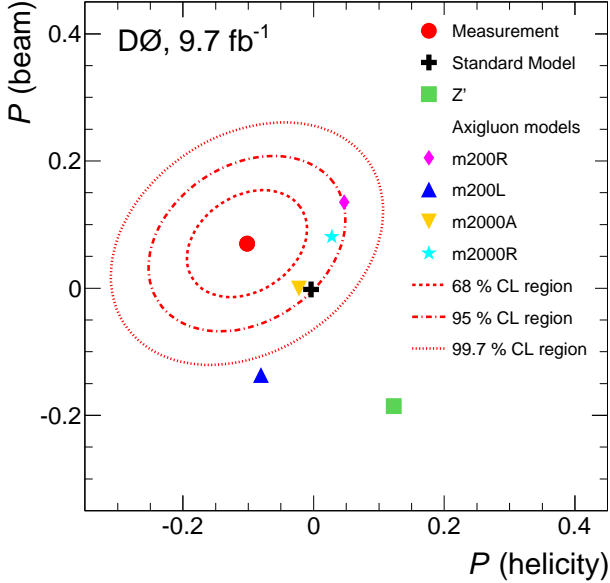


FIG. 2: (color online) Two dimensional visualization of the longitudinal top quark polarizations in the $\ell$+jets channel measured along the beam and helicity axes compared with the SM and the BSM models described in the text. In this case, the m200A model is not shown as it is indistinguishable from m2000A model. The correlation of the two measurement uncertainties is 27%.

[1] S. Fajfer, J. F. Kamenik and B. Melic, *Discerning New Physics in Top-Antitop Production using Top Spin Observables at Hadron Colliders*, JHEP **1208**, 114 (2012).

[2] W. Bernreuther and Z.-G. Si, *Distributions and correlations for top quark pair production and decay at the Tevatron and LHC*, Nucl. Phys. B **837** (2010) 90.

[3] A. Brandenburg, Z.-G. Si and P. Uwer, *QCD corrected spin analyzing power of jets in decays of polarized top quarks*, Phys. Lett. B **539** (2002) 235.

[4] W. Bernreuther, A. Brandenburg and P. Uwer, *Transverse polarization of top quark pairs at the Tevatron and the large hadron collider*, Phys. Lett. B **368** (1996) 153.

[5] M. Baumgart and B. Tweedie, *Transverse Top Quark Polarization and the $t\bar{t}$ Forward-Backward Asymmetry*, J. High Energy Phys. **1308** (2013) 072.

[6] V. M. Abazov *et al.* (D0 Collaboration), *Measurement of Leptonic Asymmetries and Top Quark Polarization in $t\bar{t}$ Production*, Phys. Rev. D **87**, 011103 (2013).

[7] V. M. Abazov *et al.* (D0 Collaboration), *Simultaneous Measurement of Forward-Backward Asymmetry and Top Polarization in Dilepton Final States from $t\bar{t}$ Production at the Tevatron*, Phys. Rev. D **92**, 052007 (2015).

[8] G. Aad *et al.* (ATLAS Collaboration), *Measurement of Top Quark Polarization in Top-Antitop Events from Proton-Proton Collisions at $\sqrt{s} = 7$ TeV Using the AT-LAS Detector*, Phys. Rev. Lett. **111**, 232002 (2013).

[9] S. Chatrchyan *et al.* (CMS Collaboration), *Measurements of $t\bar{t}$ spin correlations and top-quark polarization using dilepton final states in pp collisions at $\sqrt{s} = 7$ TeV*, Phys. Rev. Lett. **112**, 182001 (2014); V. Khachatryan *et al.* (CMS Collaboration), *Measurements of $t\bar{t}$ spin correlations and top quark polarization using dilepton final states in pp collisions at $\sqrt{s} = 8$ TeV*, Phys. Rev. D **93**, 052007 (2016).

[10] J. A. Aguilar-Saavedra, *Portrait of a colour octet*, JHEP **1408**, 172 (2014); J. A. Aguilar-Saavedra, *Missing Top Properties*, in Proceedings of the 7th International Workshop on Top Quark Physics, Cannes, France, 2014 (unpublished).

[11] D. Choudhury, R. M. Godbole, S. D. Rindani and P. Saha, *Top polarization, forward-backward asymmetry and new physics*, Phys. Rev. D **84**, 014023 (2011).

[12] W. Bernreuther, M. Fücker and Z.-G. Si, *Weak interaction corrections to hadronic top quark pair production: Contributions from quark-gluon and b anti-b induced reactions*, Phys. Rev. D **78**, 017503 (2008); W. Bernreuther and Z.-G. Si, unpublished e-mail communication.

[13] The pseudorapidity $\eta_d = -\ln[\tan(\theta/2)]$ is measured relative to the center of the detector, and $\theta$ is the polar angle with respect to the proton beam direction. The physics pseudorapidity, $\eta$, is defined using the measured polar angle of an object.

[14] V. M. Abazov *et al.* (D0 Collaboration), *The Upgraded D0 Detector*, Nucl. Instrum. Methods Phys. Res. Sec. A **565**, 463 (2006).

[15] R. Angstadt *et al.*, *The layer 0 inner silicon detector of the D0 experiment*, Nucl. Instrum. Methods Phys. Res. Sec. A **622**, 298 (2010).

[16] S. Abachi *et al.* (D0 Collaboration), *The D0 Detector*, Nucl. Instrum. Methods Phys. Res. A **338**, 185 (1994).

[17] V. M. Abazov *et al.* (D0 Collaboration), *The muon system of the Run II D0 detector*, Nucl. Instrum. Methods Phys. Res. Sec. A **552**, 372 (2005).

[18] V. M. Abazov *et al.* (D0 Collaboration), *Electron and Photon Identification in the D0 Experiment*, Nucl. Instrum. Meth. Phys. Res. Sec A **750**, 78 (2014).

[19] V. M. Abazov *et al.* (D0 Collaboration), *Muon reconstruction and identification with the Run II D0 detector*, Nucl. Instrum. Methods Phys. Res. Sec. A **737**, 281 (2014).

[20] G. C. Blazey *et al.*, *Run II jet physics*, hep-ex/0005012.

[21] V. M. Abazov *et al.* (D0 Collaboration), *Jet energy scale determination in the D0 experiment*, Nucl. Instrum. Methods Phys. Res. Sec. A **763**, 442 (2014).

[22] V. M. Abazov *et al.* (D0 Collaboration), *Improved b quark jet identification at the D0 experiment*, Nucl. Instrum. Methods Phys. Res. Sec. A **763**, 290 (2014).

[23] J. Smith, W. L. van Neerven and J. A. M. Vermaseren, *The Transverse Mass and Width of the W Boson*, Phys. Rev. Lett. **50**, 1738 (1983).

[24] V. M. Abazov *et al.* (D0 Collaboration), *Measurement of differential $t\bar{t}$ production cross sections in $p\bar{p}$ collisions*, Phys. Rev. D **90**, 092006 (2014).

[25] S. Frixione and B. R. Webber, *Matching NLO QCD computations and parton shower simulations*, JHEP **0206** (2002) 029; S. Frixione et al., *Matching NLO QCD and parton showers in heavy flavour production*, JHEP **0308** (2003) 007.

[26] M. L. Mangano, M. Moretti, F. Piccinini, R. Pittau and A. D. Polosa, ALPGEN, *a generator for hard multiparton processes in hadronic collisions*, JHEP **0307**, 001 (2003).

[27] G. Corcella et al., HERWIG *6: An Event generator for hadron emission reactions with interfering gluons (including supersymmetric processes)*, JHEP **0101**, 010 (2001).

[28] T. Sjøstrand, S. Mrenna, and P. Skands, PYTHIA *6.4 physics and manual*, J. High Energy Phys. 05 (2006) 026.

[29] R. Brun and F. Carminati, CERN Program Library Long Writeup W5013 (1993) (unpublished).

[30] E. Boos *et al.* (CompHEP Collaboration), *CompHEP 4.4: Automatic computations from Lagrangians to events*, Nucl. Instrum. Meth. A **534**, 250 (2004).

[31] V. M. Abazov *et al.* (D0 Collaboration), *Measurement of the $t\bar{t}$ production cross section in $p\bar{p}$ collisions at $\sqrt{s} = $ 1.96 TeV using secondary vertex b tagging*, Phys. Rev. D **74**, 112004 (2006).

[32] A. Carmona *et al.*, *From Tevatron's top and lepton-based asymmetries to the LHC*, JHEP **1407**, 005 (2014).

[33] J. Alwall *et al.*, *The automated computation of tree-level and next-to-leading order differential cross sections, and their matching to parton shower simulations*, JHEP **1407**, 079 (2014).

[34] V. M. Abazov *et al.* (D0 Collaboration), *Measurement of the forward-backward asymmetry in top quark-antiquark production in $p\bar{p}$ collisions using the lepton+jets channel*, Phys. Rev. D **90**, 072011 (2014).

[35] R. Demina, A. Harel and D. Orbaker, *Reconstructing $t\bar{t}$ events with one lost jet*, Nucl. Instrum. Methods Phys. Res. Sec. A **788**, 128 (2015).

[36] V. M. Abazov *et al.* (D0 Collaboration), *Measurement of the $t\bar{t}$ production cross section in $p\bar{p}$ collisions at $\sqrt{s}=1.96$ TeV using kinematic characteristics of lepton + jets events*, Phys. Rev. D **76**, 092007 (2007).

[37] M. Czakon, P. Fiedler and A. Mitov, *Resolving the Tevatron Top Quark Forward-Backward Asymmetry Puzzle: Fully Differential Next-to-Next-to-Leading-Order Calculation*, Phys. Rev. Lett. **115**, 052001 (2015).

[38] M. Czakon, P. Fiedler, D. Heymes and A. Mitov, *NNLO QCD predictions for fully-differential top-quark pair production at the Tevatron*, JHEP **1605**, 034 (2016).

[39] L. Lyons, D. Gibaut and P. Clifford, *How to Combine Correlated Estimates of a Single Physical Quantity*, Nucl. Instrum. Meth. A **270**, 110 (1988).

[40] A. Valassi, *Combining correlated measurements of several different physical quantities*, Nucl. Instrum. Meth. A **500**, 391 (2003).